Ku80 Binds to Human Replication Origins Prior to the Assembly of the ORC Complex†

Sahar Sibani,‡,§ Gerald B. Price,‡,|| and Maria Zannis-Hadjopoulos*,‡,§

McGill Cancer Center and Department of Biochemistry, McGill University, Montreal, Quebec, Canada H3G 1Y6

Received December 20, 2004; Revised Manuscript Received April 8, 2005

ABSTRACT: The Ku heterodimer, an abundant nuclear protein, binds DNA replication origins in a sequence-specific manner and promotes initiation. In this study, using HCT116 Ku80$^{+/-}$ haplo-insufficient and Orc2$^{\Delta/-}$ hypomorphic cells, the order of binding of Ku and the human *o*rigin *r*ecognition *c*omplex (HsORC) was determined. The nuclear expression of Ku80 was found to be decreased by 60% in Ku80$^{+/-}$ cells, while its general association with chromatin was decreased by 33%. Coimmunoprecipitation studies indicated that the Ku heterodimer associates specifically with the human HsOrc-2, -3, -4, and -6 subunits. *Ch*romatin *i*mmuno*p*recipitation (ChIP) experiments, using cells synchronized to late G_1, showed that the association of Ku80 with the lamin B2, β-globin, and c-*myc* origins in vivo was decreased by 1.5-, 2.3-, and 2.5-fold, respectively, in Ku80$^{+/-}$ cells. The association of HsOrc-3, -4, and -6 was consistently decreased in all three origins examined in Ku80$^{+/-}$ cells, while that of HsOrc-2 showed no significant variation, indicating that the HsOrc-3, -4, and -6 subunits bind to the origins after Ku80. In Orc2$^{\Delta/-}$ cells, the association of HsOrc-2 with the lamin B2, β-globin, and c-*myc* origins was decreased by 2.8-, 4.9-, and 2.8-fold, respectively, relative to wild-type HCT116 cells. Furthermore, nascent strand abundance at these three origins was decreased by 4.5-, 2.3-, and 2.6-fold in Orc2$^{\Delta/-}$ relative to HCT116 cells, respectively. Interestingly, the association of Ku80 with these origins was not affected in this hypomorphic cell line, indicating that Ku and HsOrc-2 bind to origins independently of each other.

Initiation of DNA replication occurs within specific initiation regions at defined sequences called origins (*1*−*8* and references cited therein). Although origin activation may be modified by chromatin structure (*9*), the isolation of origins allowed purification of initiator proteins of DNA replication (*10*−*12*). The first group of such proteins to be purified was the *o*rigin *r*ecognition *c*omplex from *Saccharomyces cerevisiae* (ScORC), through its ability to bind to the *ARS c*onsensus *s*equence (ACS or A-site) present at the *ARS*1 origin (*10*). ScORC consists of six polypeptide subunits (ScOrc1−6), and, in the presence of ATP, displays sequence-specific binding to *ARS*1 via the ScOrc1p subunit (*10*, *13*). More recent studies using the human homologue of the ORC[1] complex (HsORC), expressed in a baculovirus system, showed that it lacked sequence-specific DNA binding activity (*14*−*16*). However, *ch*romatin *i*mmuno*p*recipitation assays (ChIP) using antibodies raised against different HsORC subunits pulled down specific DNA sites in vivo, indicating that the in vivo interaction of HsORC with DNA is not random (*16*). ChIP experiments using anti-HsOrc1 and -HsOrc2 led to the identification of a novel origin of replication located in the intergenic region between the *PRKDC* and *MCM4* genes in HeLa cells (*16*). In another ChIP experiment using HsOrc2 as the precipitating protein, a novel origin in the human TOP1 promoter was identified (*17*). Furthermore, ChIP analysis of the association of HsOrc2 with a plasmid containing the replication origin of Epstein−Barr virus (EBV), OriP, indicated a specific association with the dyad symmetry sequence (*18*−*21*). These results suggested that another protein may be involved in sequence-specific origin binding in human cells (*15*, *22*, *23*), subsequently recruiting HsORC to human origins of DNA replication. Recent studies have identified Ku80 as a potential candidate, i.e., a novel initiator protein, participating in site-specific origin binding (*11*, *12*, *23*−*25*). Ku80 is the 80 kDa subunit of the heterodimeric Ku protein, which consists of the Ku70 and Ku80 subunits (reviewed in ref *26*).

Ku was initially isolated as an autoantigen from systemic lupus erythematosus patients and has been implicated in various DNA-related cellular functions, including DNA repair, recombination, replication, transcriptional silencing, and telomere maintenance (reviewed in refs *22* and *26*). The Ku heterodimer was purified through its ability to bind directly to an origin-derived sequence, A3/4 (*11*, *12*), a version of a mammalian origin consensus sequence (*27*). Southwestern analyses revealed that Ku80 was the origin-binding subunit (*12*), while in vitro footprinting revealed that the heterodimer bound to A3/4 in a sequence-specific manner (*28*). ChIP analyses indicated that Ku associates specifically with DNA replication origins in vivo in a cell cycle

† This research was supported by grants from the CIHR (M.Z.-H.) and the Cancer Research Society (G.B.P.). S.S. was a recipient of doctoral studentships from the CIHR/K. M. Hunter Charitable Foundation, the FCAR/FRSQ, and McGill University.

* To whom correspondence should be addressed. Tel: (514) 398-3536. Fax: (514) 398-6769. E-mail: maria.zannis@mcgill.ca.

‡ McGill Cancer Center.

§ Department of Biochemistry.

|| In memoriam.

[1] Abbreviations: ChIP, chromatin immunoprecipitation; EBV, Epstein−Barr virus; ORC, origin recognition complex; NGS, normal goat serum; NRS, normal rabbit serum; pre-RC, prereplication complex.

10.1021/bi047327n CCC: $30.25
Published on Web 05/07/2005

dependent manner, its association being maximal in late G_1 and decreasing as cells enter S phase (*23*). Immunodepletion of Ku from HeLa cell extracts resulted in a 70% decrease in in vitro DNA replication (*12*), while coimmunoprecipitation studies indicated that Ku interacts with other DNA replication proteins, including HsOrc2, DNA polymerases α, δ, and ϵ, PCNA, topoisomerase II, RFC, and RPA (*24*). Ku80$^{-/-}$ mouse embryonic fibroblasts (MEF) have a prolonged doubling time compared to the wild-type cells, exhibit premature senescence, and fail to proliferate in culture (*29*). Human HCT116 Ku80$^{-/-}$ cells are nonviable, while HCT116 Ku80$^{+/-}$ haplo-insufficient cells have a prolonged doubling time of 20.5 h versus 17.7 h for the wild-type cells (*30*) and display a prolonged G_1 phase (*31*). The association of both Ku subunits (Ku70 and Ku80) with origins of DNA replication was decreased in the HCT116 Ku80$^{+/-}$ cells, as was the replication origin activity (*31*).

In this study, HCT116 cells deficient of the essential proteins Ku and Orc2 were used to carry out an epistatic analysis to determine the order of association of Ku80 and HsOrc-2, -3, -4, and -6 with replication origins in vivo. The data show that Ku80 and HsOrc2 bind to origins independently of each other, while the binding of Ku precedes that of HsOrc-3, -4, and -6.

MATERIALS AND METHODS

Cell Culture and Synchronization. HCT116 and Ku80$^{+/-}$ (clone 70-32; generous gift from Dr. Eric A. Hendrickson) cells were previously described (*30*). Briefly, one Ku80 allele was knocked out using Cre-loxP technology, resulting in deletion of the *Ku80* promoter and exon 1. Orc2$^{\Delta/-}$ hypomorphic cells (a generous gift from Dr. Anindya Dutta) were generated by deletion of exon 3, which harbors the initiating ATG, from both alleles (*18*). All cell lines were cultured in αMEM (minimum essential medium) (Invitrogen, Carlsad, CA) supplemented with 10% fetal bovine serum (FBS; Invitrogen) (hereafter termed complete medium) at 37 °C and 5% CO_2. Synchronization to late G_1 phase was carried out as previously described (*23*). Briefly, cells were cultured in complete medium in the presence of 2 mM thymidine (Sigma, St. Louis, MO) for 12 h, released for 10 h in prewarmed complete medium without thymidine, and then incubated for 12−14 h in complete medium containing 400 μM mimosine (Sigma). Cell synchronization was monitored by flow cytometry (*32*).

Preparation of Nuclear Extracts and Chromatin-Enriched Fractions. Nuclear extracts were prepared by the Dignam method, as previously described (*33*). Chromatin-enriched extracts were also prepared according to standard methods, as described in ref *34*. The protein concentration of each extract preparation was determined by the Bradford protein assay, according to the manufacturer's protocol (Bio-Rad, Hercules, CA).

Western and Immunoblot Analyses. Western blot analysis was carried out according to standard protocol (*35*). The indicated amounts of protein extracts were subjected to electrophoresis on a 5% stacking/8% separating SDS−PAGE gel, followed by transfer to a PVDF membrane and blocking with 5% skim milk. Membranes were incubated with a 1/100 dilution of goat anti-Ku80 (C-20; Santa Cruz Biotechnology, Santa Cruz, CA) or a 1/2500 dilution of either rabbit anti-HsOrc-2, -3, -4, or -6 antibody (generous gifts from Dr. Anindya Dutta) (*36*) for 1 h at room temperature. Finally, they were incubated with a 1/2000 dilution of either anti-goat or anti-rabbit horseradish peroxidase (HRP) conjugated IgG for 20 min at room temperature (Santa Cruz Biotechnology). Immunoblots were also probed with a 1/1000 dilution of anti-actin (Sigma) or anti-MCM7 antibodies (N-20; Santa Cruz Biotechnology), as loading controls. Proteins were visualized using the ECL system (Amersham Biosciences Inc., Arlington Heights, IL), and signals were quantified using FujiFilms Image Gauge V3.3.

Chromatin Immunoprecipitation Assay (ChIP). The ChIP assay was carried out exactly as described previously (*23*, *37*). Half of the immunoprecipitated material was used for western blot analysis, while DNA was extracted from the remaining half, as previously described (*23*), resuspended in 100 μL of ddH_2O, and used for real-time PCR quantification.

Nascent DNA Preparation. Nascent DNA was prepared from asynchronous cultures grown in complete media as described in ref *38*. Briefly, cells cultured in five 15 cm plates were lysed with 5 mL of Hirt lysis buffer each (50 mM Tris-HCl, pH 8.0, 0.6 M NaCl, 1 mM EDTA, 0.5% SDS) (*39*). The lysates were digested with 0.1 mg/mL proteinase K overnight at 37 °C, and nucleic acids were extracted by the standard phenol−chloroform method (*35*). Twenty micrograms of heat-denatured DNA was phosphorylated by T4PNK (NEB) with 1 mM ATP and digested with 15 units of λ-exonuclease overnight at 37 °C. λ-Exonuclease digests any DNA in the 5′ to 3′ direction, but not RNA; thus nascent DNA strands with 5′ RNA primers are protected, while parental DNA is not. The digested DNA was then heat denatured at 95 °C for 10 min and subjected to electrophoresis on a native agarose gel. DNA was visualized with methylene blue, and fragments of 0.5−1 kb in size, which are enriched in origin-containing nascent DNA, were extracted from the gel using the QiaQuick gel extraction kit (Qiagen), according to manufacturer's instructions, and eluted in 250 μL of ddH_2O. The concentration of nascent DNA was assessed using real-time PCR.

Real-Time PCR Quantification of Immunoprecipitated or Nascent DNA. The LightCycler instrument (Roche Diagnostics, Basel, Switzerland) along with the LightCycler FastStart DNA Master SYBR Green I kit (Roche Molecular Biochemicals, Indianapolis, IN) was used to quantify either nascent DNA or immunoprecipitated DNA obtained from the ChIP assay, according to the manufacturer's instructions. Briefly, 2 μL of a 10× Master mix was combined with 2 μL of either nascent or ChIP DNA and 1 μM primer in a total volume of 20 μL. An initial 10 min denaturation step at 99 °C was used, followed by 40 cycles of the following cycling conditions: 99 °C for 10 s, annealing temperature (as indicated in Table 1) for 10 s, and 72 °C for 15 s. The sequence and locations of all primer sets used are listed in Table 1. None of the primer sets produced nonspecific PCR products.

Each PCR run was calibrated using serial dilutions of genomic DNA to generate a standard curve of fluorescence emitted by each PCR amplicon (Figure 4B). The genomic DNA was extracted from serum-starved, nonreplicating HCT116 cells, thus providing a diploid genome. The

Table 1: Sequences and Annealing Temperatures of Primers Used for the LightCycler[a]

primer name	sequence (5′ → 3′)	$T_{annealing}$ (°C)	GenBank accession no.	location of primer (5′ → 3′)
LB2F	GGCTGGCATGGACTTTCATTTCAG	66	M94363	3839−3862
LB2R	GTGGAGGGATCTTTCTTAGACATC			4070−4047
LB2C1F	GTTAACAGTCAGGCGCATGGGCC	66		1−23
LB2C1R	CCATCAGGGTCACCTCTGGTTCC			240−217
BG40.9F	AATCTATTCTGCTGAGAGATCACAC	62	455025	40963−40987
BG40.9R	CCACTTGCAGAACTCCCGTGTAC			41195−41173
BG72F	GTCTAAAACACCAAAACGAATGGCAAC	55		72152−72178
BG72R	CATTTCTCTGATGGCTAGTGATGATGAG			72478−72451
*Myc*11F	TATCTACACTAACATCCCACGCTCTG	62	AC103819	87125−87150
*Myc*11R	CATCCTTGTCCTGTGAGTATAAATCATCG			87345−87317
*Myc*1F	TTCTCAACCTCAGCACTGGTGACA	68		80946−80969
*Myc*1R	GACTTTGCTGTTTGCTGTCAGGCT			81246−81222

[a] Names and sequences of primers used for real-time quantification of DNA using the LightCycler (Roche Diagnositics) are listed above. The names are identical to the region amplified (see Figure 4A) and are followed by F or R to designate the forward and reverse primers, respectively. The $T_{annealing}$ is the annealing temperature used in the cycling conditions for the LightCycler. Locations of the primers within the indicated GenBank accession entry are indicated.

fluorescence emitted by each sample was then charted onto the standard curve, and the amount of DNA within each sample was determined and converted to molecules using the formula:

$$\frac{(\text{DNA amount})(\text{Avogadro's number})(\text{dilution factor})}{(\text{molecular weight of amplicon})}$$

where DNA amount is given in micrograms, Avogadro's number is 6×10^{23} molecules/mol, dilution factor is derived by dividing the elution volume (100 μL for ChIP and 250 μL for nascent DNA) by the volume of sample added to each PCR reaction (2 μL), and the molecular weight (grams per mole) was calculated by multiplying 660 (g/mol × bp) by the length of the amplicon (in bp).

RESULTS

Decreased Expression of Ku80 Protein in Ku80$^{+/-}$ Cells Does Not Affect Expression of the HsOrc Proteins. Analysis of the nuclear expression of Ku80 in HCT116 Ku80$^{+/-}$ cells revealed a 60% decrease by comparison to their wild-type counterparts (Figure 1; $p = 0.03$). In a parallel study, the expression of Ku70 was found to be decreased by 36% in Ku80$^{+/-}$ cells (*31*). In contrast, a similar analysis of the expression of the HsOrc-2, -3, -4, and -6 subunits showed no significant differences between the wild-type and Ku80-deficient HCT116 cells (Figure 1; $p > 0.05$), indicating that Ku is not required for either the expression or stability of the HsOrc subunits. Actin was used as a loading control (Figure 1A), and no significant differences were obtained between the two cell lines (Figure 1B).

General Chromatin Loading of the HsOrcs Is Not Affected by Ku80 Deficiency. To examine the effect of Ku80 deficiency on the association of Ku80 and ORC with chromatin, western blot analyses of chromatin-enriched fractions from Ku80$^{+/-}$ and HCT116 cells were carried out, using anti-Ku80 and anti-Orc antibodies (Figure 2). As expected, the association of Ku80 with chromatin was decreased in the deficient cells relative to their wild-type counterparts (Figure 2A). Quantification of the obtained bands revealed a significant decrease of approximately 33% ($p = 0.0035$) (Figure 2B). Ku70 was also decreased in the Ku80$^{+/-}$ cells by 40% ($p = 0.01$) (*31*). Similar analysis of

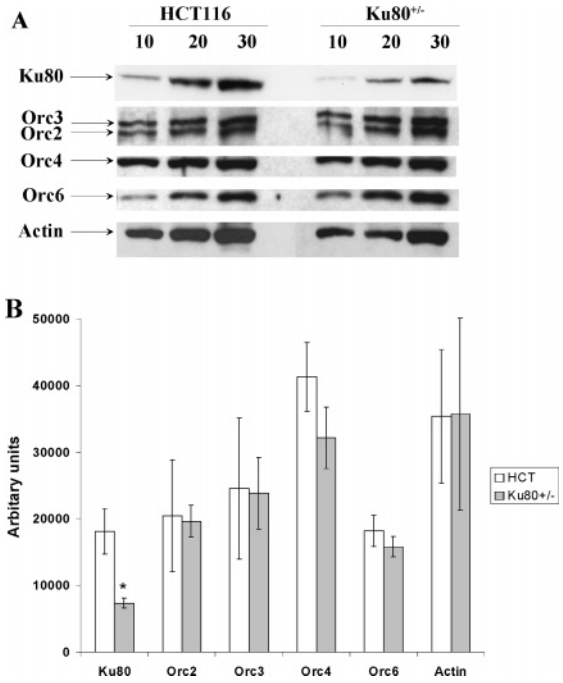

FIGURE 1: Western blot analysis and quantification of Ku80 and HsOrc-2, -3, -4, and -6 in nuclear extracts of wild-type HCT116 and Ku80$^{+/-}$ cells. (A) Nuclear extracts were prepared from log phase cells by the Dignam method (see Materials and Methods). Increasing amounts (10, 20, or 30 μg) of nuclear extracts from wild-type HCT116 or Ku80$^{+/-}$ cells were immunoblotted for Ku80 and HsOrc-2, -3, -4, and -6. Actin was used as a loading control. (B) Quantification of the bands shown in panel A. Error bars represent the average of three experiments and one standard deviation. The asterisk represents statistically significant ($p < 0.05$) differences in protein expression between HCT and Ku80$^{+/-}$ cells.

HsOrc-2, -3, -4, and -6 loading onto chromatin did not reveal any significant differences between the HCT116 and Ku80$^{+/-}$ cells ($p > 0.05$) (Figure 2). MCM7, a member of the putative DNA replication helicase, was used as a loading control, and its association with chromatin was found to be the same in the two cell lines.

Ku and HsOrc Proteins Coimmunoprecipitate. Since both Ku and HsORC have been implicated in the initiation of DNA replication (*24*, *25*, and *40* and references cited therein) and the Ku heterodimer has been shown to coimmunoprecipitate with HsOrc2, but not HsOrc1, in nuclear extracts

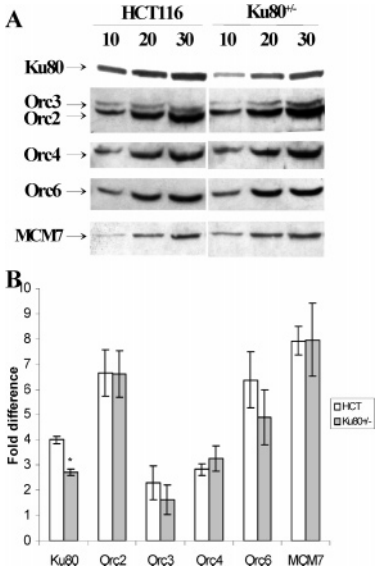

FIGURE 2: Chromatin loading of Ku80 and HsOrc-2, -3, -4, and -6 in wild-type HCT116 and Ku80$^{+/-}$ cells. Chromatin-enriched fractions were prepared from HCT116 and Ku80$^{+/-}$ cells by DNase I nuclease digestion of Triton X-100 treated cells. (A) Increasing amounts (10, 20, and 30 μg) of these fractions were immunoblotted for Ku80 and HsOrc-2, -3, -4, and -6. MCM7 was used as a loading control. (B) Quantification of the bands shown in panel A, normalized relative to MCM7. Error bars represent the average of three experiments and one standard deviation.

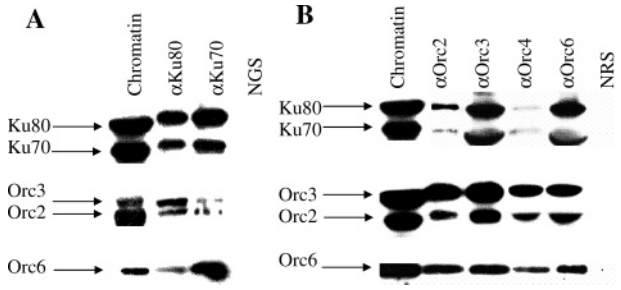

FIGURE 3: Coimmunoprecipitation of Ku and HsOrc proteins in chromatin-enriched fractions. (A) Chromatin-enriched fractions were immunoprecipitated with either anti-Ku80 or anti-Ku70 antibodies, or normal goat (NGS) or rabbit serum (NRS), as indicated at the top of the figure. The input chromatin fraction is shown in the first lane. The immunoprecipitates were immunoblotted for Ku80, Ku70, and HsOrc-2, -3, and -6, as indicated on the left. HsOrc4 is not shown because of its comigration with the heavy chain of IgG. (B) Same as in (A), except anti-HsOrc-2, -3, -4, and -6 antibodies were used for the immunoprecipitations (indicated at the top of the figure). For both panels, two blots were made: one probed with the two anti-Ku antibodies and the other with the three anti-Orc antibodies. Lack of cross-reactivity of the antibodies had been previously verified.

(*24*), we examined the interactions between the Ku and HsORC subunits in chromatin-enriched extracts of wild-type HCT116 cells. Following formaldehyde cross-linking to stabilize any existing interactions, the samples were sonicated to shear the DNA, thus preventing coprecipitation of proteins due to their association to the same DNA fragment. Anti-Ku80 and anti-Ku70 antibodies were then used for immunoprecipitation, and the precipitates were analyzed by immunoblotting for the presence of the target proteins (Figure 3A). Both antibodies precipitated their respective target Ku proteins and coprecipitated the HsOrc-2, -3, and -6 proteins (Figure 3A, lanes 2 and 3). In contrast, when normal goat serum (NGS) was used in place of the anti-Ku antibodies, none of these proteins were brought down, indicating that the washes were of sufficient stringency to prevent detection of nonspecific interactions (Figure 3A, lane 4). Coimmunoprecipitation of HsOrc4 could not be analyzed because of its comigration with the heavy chain of IgG of the immunoprecipitating anti-Ku antibodies (not shown).

To confirm the specificity of the coimmunoprecipitations, the reverse reactions were also performed in which anti-HsOrc-2, -3, -4, and -6 antibodies were used in the immunoprecipitations, followed by immunoblotting for the two Ku subunits (Figure 3B). Each of the anti-HsOrc antibodies immunoprecipitated its target protein as well as the other members of the HsORC complex (Figure 3B, lanes 2−5). Furthermore, all anti-HsOrc antibodies coimmunoprecipitated both Ku70 and Ku80 (Figure 3B, lanes 2−5), indicating that the Ku heterodimer and HsORC proteins are part of a complex. Although immunoblotting for HsOrc4 was not possible due to its comigration with the IgG heavy chain, the presence of the other HsOrc and Ku subunits in the immunoprecipitate obtained using anti-HsOrc4 antibody (Figure 3B, lane 4) indirectly indicated that HsOrc4 was also immunoprecipitated. None of these DNA replication proteins were immunoprecipitated by NRS, once again indicating that the observed interactions were specific (Figure 3B, lane 6).

Decreased HsOrc Association with Origins of DNA Replication in Ku80$^{+/-}$ Cells. In view of the unchanged profiles of the association of HsOrc-2, -3, -4, and -6 proteins with chromatin in Ku80$^{+/-}$ cells, we examined whether there was a difference in the association of these proteins with replication origins in vivo. Using the chromatin immunoprecipitation (ChIP) assay and quantitative real-time PCR, three early replicating origins were examined: lamin B2, β-globin, and c-*myc* (Figure 4A). For each of these origins, quantitative PCR amplification was carried out at the peak initiation region as well as at a region lacking origin activity, henceforth referred to as a negative region. Thus, LB2 and LB2C1 are the peak and negative regions of the lamin B2 origin, respectively, as previously defined (*41*, *42*), and BG40.9 and BG72 are the peak and negative regions for the β-globin origin, respectively (*43*). The choice of the Aγ origin (Figure 4A), instead of a more distal origin in the β-globin gene locus, was based on published data showing greater abundance of nascent DNA at the Aγ region in HCT116 cells (*43*). Finally, the major initiation site of nascent DNA replication at the c-*myc* locus, *Myc*1, and its negative region, *Myc*1, were also analyzed (Figure 4A) (*38*).

Quantification by real-time PCR using the LightCycler required the use of standard curves for each amplified region (Figure 4B). The regression coefficient (r^2 value) for all graphs ranged between 0.98 and 1.00, denoting a good linear correlation, and the slopes of all the standard curves were similar (ranging from −3.228 to −4.230), indicating similar amplification efficiencies for all primer sets, thus permitting quantitative comparisons between different primer pairs.

As expected, in mimosine-arrested Ku80$^{+/-}$ cells, ChIP analysis of Ku80 showed its decreased association with all three origins (Figure 5). Comparing the abundance of Ku80-immunoprecipitated DNA molecules between the HCT116 wild-type and Ku80$^{+/-}$ cells, the lamin B2 origin, LB2, showed approximately a 1.5-fold decrease (2.4×10^6 vs 1.6×10^6 molecules/2×10^7 cells, respectively, $p = 0.003$), while the β-globin and c-*myc* origins had approximately a

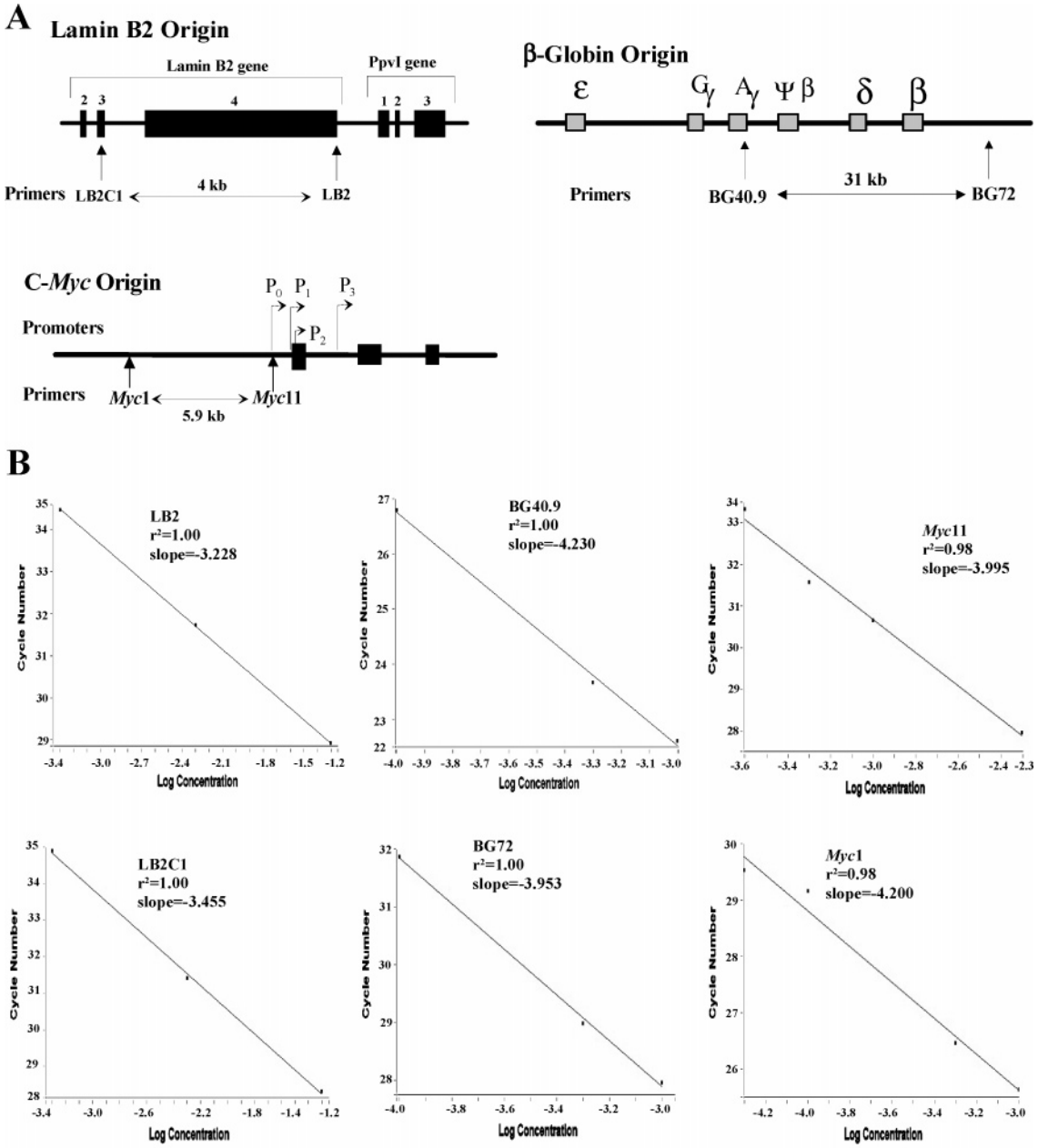

FIGURE 4: The lamin B2, β-globin, and c-*myc* origins. (A) Schematic maps of the lamin B2, β-globin, and c-*myc* origins, showing the locations of the PCR-amplified regions (upward arrows). For the lamin B2 locus, the black numbered boxes are the exons of the *Lamin B2* and *Ppv*I genes, as indicated. For the β-globin locus, the gray boxes represent the different globin genes, designated above each box. The exons of the c-*myc* gene locus (black boxes) and the four gene promoters (P0, P1, P2, and P3) are indicated. The origin-containing regions are LB2, BG40.9, and *Myc*11, and their respective negative control regions are LB2C1, BG72, and *Myc*1 for the lamin B2, β-globin, and c-*myc* origins, respectively. The double-headed arrows indicate the distance (in kb) between the positive and negative regions within each map. (B) Standard curves used for the quantification of the lamin B2 (LB2 and LB2C1), β-globin (BG40.9 and BG72), and c-*myc* (*Myc*11 and *Myc*1) amplicons are shown. The log of the DNA concentration (*X*-axis) is plotted against the cycle number at which the log-linear phase started (*Y*-axis). The regression coefficients, as well as the slope of each curve, are indicated.

2.3- and 2.5-fold decrease, respectively (13.5×10^5 vs 6×10^5 molecules/2×10^7 cells, $p = 0.025$, and 2.1×10^6 vs 8.3×10^5 molecules/2×10^7 cells, $p = 0.03$, respectively) in Ku80$^{+/-}$ cells. A similar comparison of the association of HsOrc-3, -4, and -6 with the three origins in the two cell lines showed a decrease in Ku80$^{+/-}$ cells. Thus, in the case of the lamin B2 origin (Figure 5A), the association of HsOrc-3, -4, and -6 was decreased by 1.9-, 1.7-, and 1.8-fold in Ku80$^{+/-}$ cells, respectively (3.8×10^6 vs 2.1×10^6 molecules/2×10^7 cells $p = 0.02$, for HCT116 and Ku80$^{+/-}$ cells, respectively, 1.8×10^6 vs 1.0×10^6 molecules/2×10^7 cells, $p = 0.002$, and 3.7×10^6 vs 2×10^6 molecules/2×10^7 cells, $p = 0.01$, respectively). In contrast, the association of HsOrc-2 with the lamin B2 origin was not affected by Ku80's deficiency (1.3×10^6 vs 1.3×10^6 molecules/2×10^7 cells, $p = 0.68$). For the β-globin origin (Figure 5B), BG40.9, the associations of HsOrc-3, -4, and -6 subunits were significantly decreased in Ku80$^{+/-}$ cells relative to wild-type HCT116 by approximately 1.3-, 1.9-, and 1.8-fold, respectively (2.5×10^6 vs 2×10^6 molecules/2×10^7 cells, for HCT and Ku80$^{+/-}$ cells, respectively, $p = 0.046$, 1.4×10^6 vs 7.2×10^5 molecules/2×10^7 cells, $p = 0.002$, and 2.7×10^6 vs 1.5×10^6 molecules/2×10^7 cells, $p = 0.033$, respectively). The association of HsOrc2 to

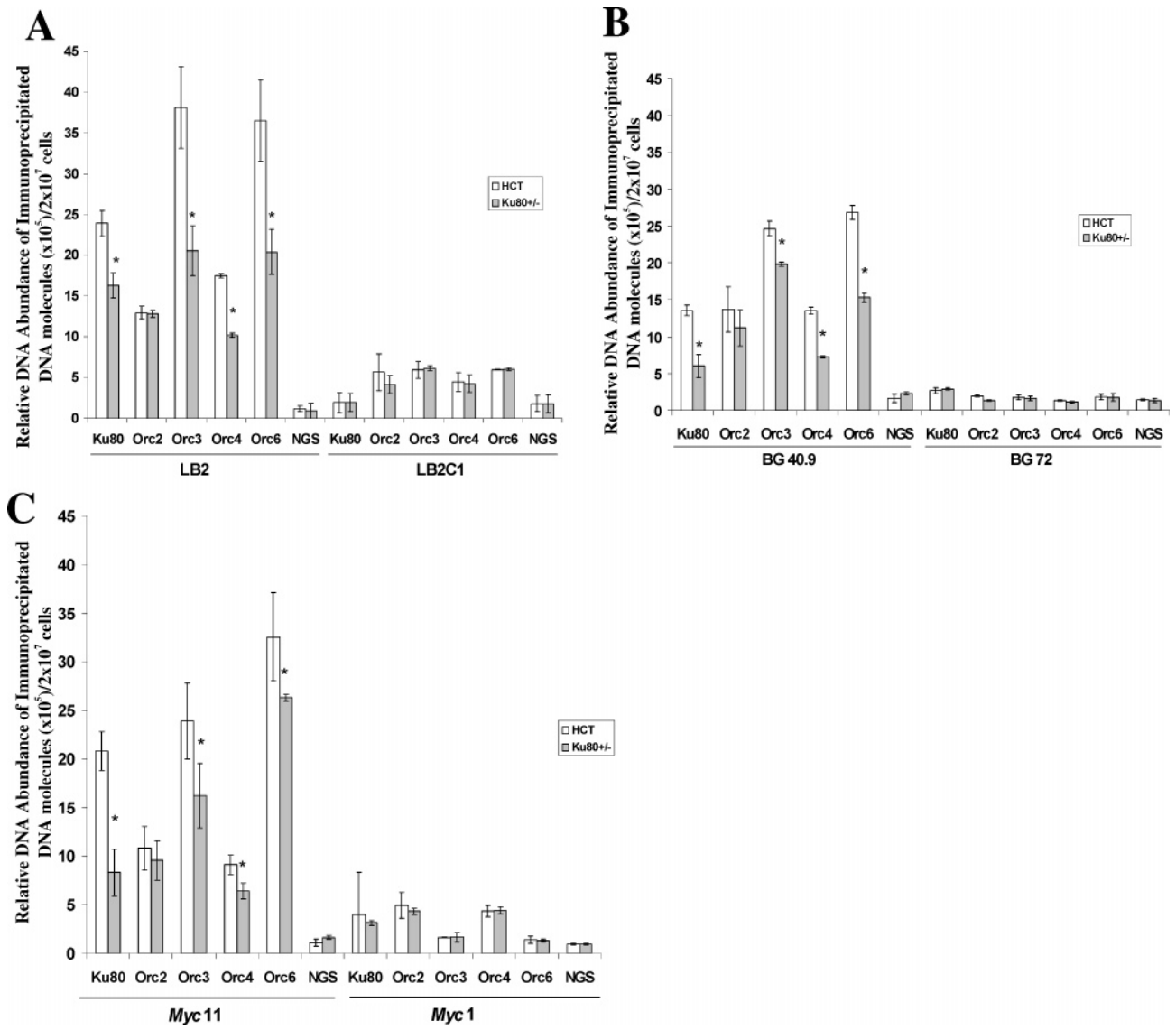

FIGURE 5: ChIP assay of Ku80 and HsOrc-2, -3, -4, and -6 in wild-type HCT116 and Ku80$^{+/-}$ cells. Chromatin immunoprecipitates were prepared from mimosine-arrested cells (as described in Materials and Methods). The abundance of DNA molecules immunoprecipitated by the anti-Ku80 and anti-HsOrc-2, -3, -4, and -6 antibodies for the lamin B2 (A), β-globin (B), and c-*myc* (C) origins of HCT116 (white bars) and Ku80$^{+/-}$ (gray bars) cells is shown. The DNA abundance of the origin-containing (LB2, BG40.9, and *Myc*11) and origin-lacking (LB2C1, BG72, and *Myc*1) regions is indicated. Normal goat serum (NGS) was used as a negative control. Error bars represent the average of three experiments, each done in duplicate, and one standard deviation. Statistically significant differences ($p < 0.05$) between ChIPs from HCT116 and Ku80$^{+/-}$ cells are indicated by an asterisk.

BG40.9 was decreased by 1.2-fold, although this was not statistically significant (1.4×10^6 vs 1.1×10^6 molecules/2 $\times 10^7$ HCT and Ku80$^{+/-}$ cells, respectively, $p = 0.47$). Finally, the c-*myc* origin (Figure 5C) showed a pattern of HsOrc association similar to that of the lamin B2 origin; that is, overall, the association of HsOrc-2 was not significantly decreased in Ku80$^{+/-}$ cells by comparison to the wild-type cells (1.1×10^6 vs 9.6×10^5 molecules/2 $\times 10^7$ cells for HCT116 and Ku80$^{+/-}$ cells, respectively, $p = 0.52$), while that of HsOrc-3, -4, and -6 was decreased by 1.5-, 1.4-, and 1.2-fold in Ku80$^{+/-}$ cells, respectively (2.4×10^6 vs 1.6×10^6 molecules/2 $\times 10^7$ cells, $p = 0.02$, 9.1×10^5 vs 6.4×10^5 molecules/2 $\times 10^7$ cells, $p = 0.02$, 3.3×10^6 vs 2.6×10^6 molecules/2 $\times 10^7$ cells, $p = 0.03$, for HCT116 and Ku80$^{+/-}$ cells, respectively).

DNA immunoprecipitated by NGS was significantly lower than that brought down by the individual anti-Ku and anti-HsOrc antibodies, indicating that the interactions depicted by these antibodies were specific (Figure 5, NGS). The average DNA abundance of NGS immunoprecipitates was 1.1×10^5, 1.9×10^5, and 1.4×10^5 molecules/2 $\times 10^7$ cells for the lamin B2, β-globin, and c-*myc* origins, respectively, while their respective origin-lacking regions were abundant at an average of 1.8×10^5, 1.4×10^5, and 1.0×10^5 molecules/2 $\times 10^7$ cells for LB2C1, BG72, and *Myc*1, respectively. Quantification of immunoprecipitated DNA for the control regions, LB2C1, BG72, and *Myc*1, did not reveal significant differences between HCT116 and Ku80$^{+/-}$ cells (Figure 5), indicating that the DNA extraction and immunoprecipitations were of comparable efficiency in the two cell lines. Ku80 immunoprecipitates averaged 1.9×10^5, 2.8×10^5, and 3.6×10^5 molecules/2 $\times 10^7$ cells for LB2C1, BG72, and *Myc*1, respectively. The immunoprecipitates of the HsOrc antibodies at LB2C1 ranged between 4.2 and 6 $\times 10^5$ molecules/2 $\times 10^7$ cells, while BG72 and *Myc*1 had

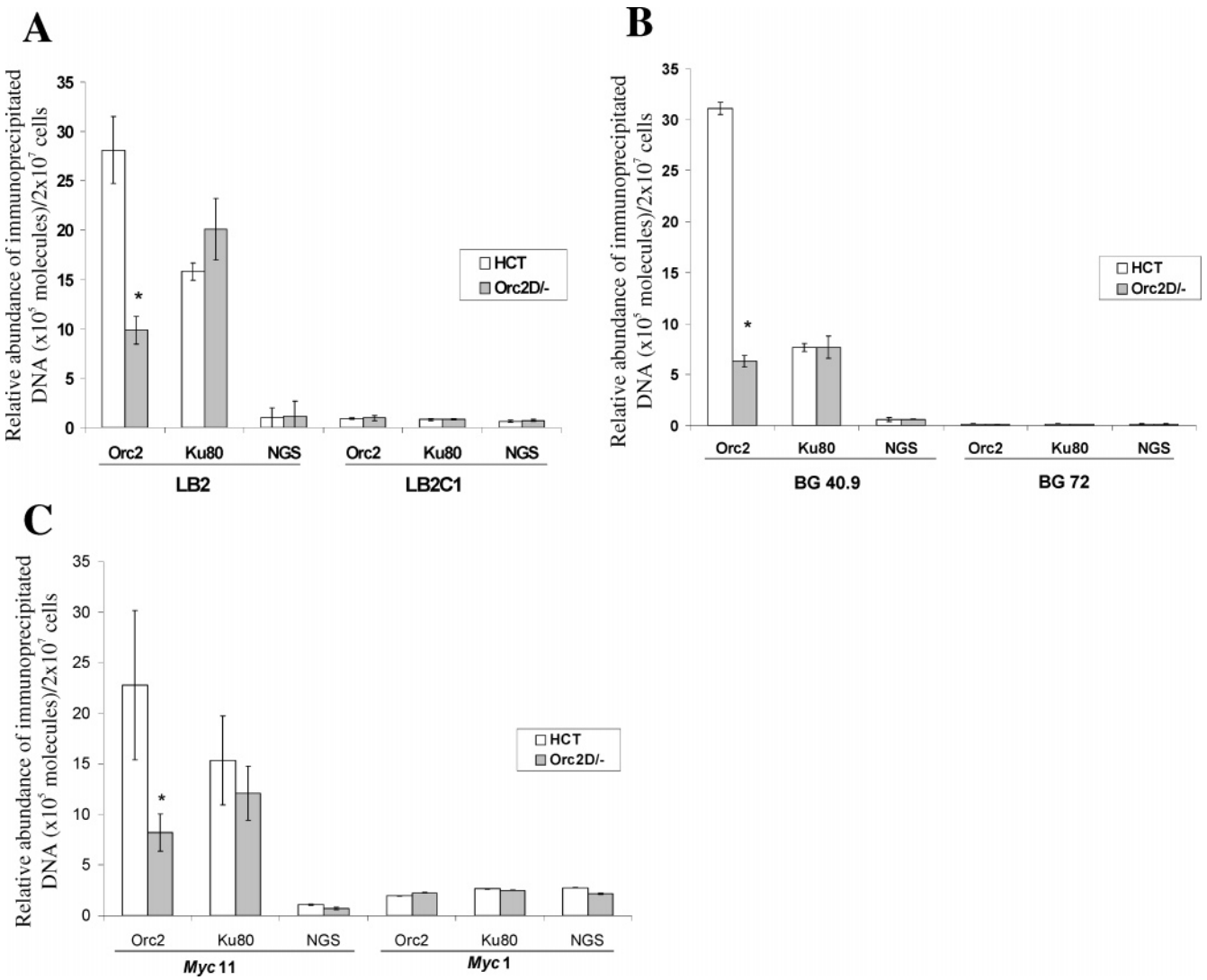

FIGURE 6: ChIP assay of Ku80 and HsOrc2 in wild-type HCT116 and Orc2$^{\Delta/-}$ cells. The abundance of DNA molecules immunoprecipitated with anti-Ku80 or anti-HsOrc2 antibodies at the lamin B2 (A), β-globin (B), and c-*myc* (C) origins in log phase wild-type HCT116 (white bars) and Orc2$^{\Delta/-}$ (gray bars) cells is shown. For each immunoprecipitate, the abundance of both the origin-containing (LB2, BG40.9, and *Myc*11) and origin-lacking (LB2C1, BG72, and *Myc*1) regions was determined. Normal goat serum (NGS) was used as a negative control. Each bar represents the average of three experiments, each done in duplicate, and one standard deviation. Statistically significant differences ($p < 0.05$) between ChIPs from HCT116 and Orc2$^{\Delta/-}$ are indicated with an asterisk.

a lower abundance of DNA molecules (1.2−2.0 $\times$ 10^5 and 1.4−4.9 $\times$ 10^5 molecules/2 $\times$ 10^7 cells, respectively).

HsOrc2 Deficiency Does Not Influence Ku80's Association with Replication Origins. HsOrc2 associates with chromatin throughout the cell cycle and is believed to be one of the first subunits of the HsORC complex to bind to replication origins (*22*, *44*, *45*). Hence, the effect of HsOrc2 deficiency on the ability of Ku80 to bind replication origins was examined to determine the order of binding of HsOrc2 and Ku (i.e., whether HsOrc2 bound to origins prior to Ku80). Comparative ChIP analysis of the association of HsOrc2 with the three aforementioned origins in asynchronously growing cultures of HCT116 wild-type and Orc2$^{\Delta/-}$ cells showed an overall decrease in the association of HsOrc2 with the origins in the hypomorphic cells (Figure 6). Specifically, the Orc2$^{\Delta/-}$ cells showed a 2.8-, 4.9-, and 2.8-fold decrease in the association of HsOrc2 with the LB2 (2.8 $\times$ 10^6 vs 9.9 $\times$ 10^5 molecules/2 $\times$ 10^7 cells, $p = 0.018$, Figure 6A), BG40.9 (3.1 $\times$ 10^6 vs 6.3 $\times$ 10^5 molecules/2 $\times$ 10^7 cells, $p = 0.004$, Figure 6B), and *Myc*11 (2.3 $\times$ 10^6 vs 8.2 $\times$ 10^5 molecules/2 $\times$ 10^7 cells, $p = 0.017$, Figure 6C) origins, respectively. The association of Ku80, on the other hand, showed neither a consistent nor significant difference in the hypomorphic Orc2$^{\Delta/-}$ cells for any of the three origins examined (1.6 $\times$ 10^6 vs 2 $\times$ 10^5 molecules/2 $\times$ 10^7 cells for LB2, $p = 0.17$, Figure 6A; 9.9 $\times$ 10^5 vs 7.7 $\times$ 10^5 molecules/2 $\times$ 10^7 cells for BG40.9, $p = 0.99$, Figure 6B; and 1.5 $\times$ 10^6 vs 1.2 $\times$ 10^6 molecules/2 $\times$ 10^7 cells for *Myc*11, $p = 0.47$, Figure 6C). As before, DNA brought down nonspecifically by normal goat serum (NGS) did not vary between the wild-type HCT116 and hypomorphic Orc2$^{\Delta/-}$ cells and averaged 1.1 $\times$ 10^5, 0.6 $\times$ 10^5, and 0.9 $\times$ 10^5 molecules/2 $\times$ 10^7 cells for LB2, BG40.9, and *Myc*11, respectively. Likewise, the abundance of the control DNA immunoprecipitated by the individual antibodies did not vary significantly from that of NGS and ranged between 0.7 $\times$ 10^5, 0.1−0.2 $\times$ 10^5, and 2.0−2.8 $\times$ 10^5 molecules/2 $\times$ 10^7 cells for LB2C1, BG72, and *Myc*1, respectively (Figure 6).

Orc2$^{\Delta/-}$ Cells Display Decreased Origin Activity. Since Ku80 deficiency decreased the association of Orc-3, -4, and

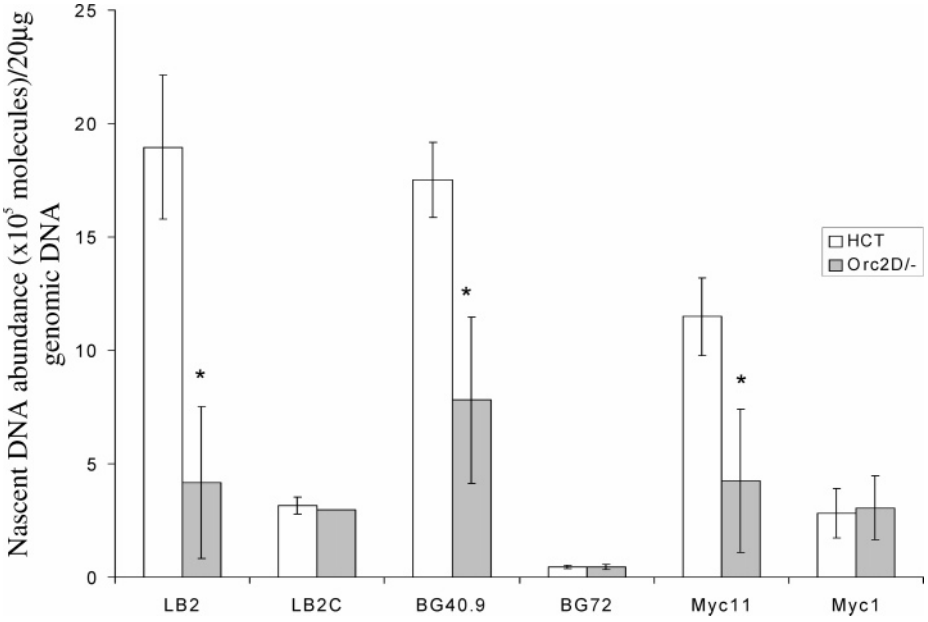

FIGURE 7: Nascent DNA abundance at the lamin B2, β-globin, and c-*myc* origins in Orc2$^{\Delta/-}$ and HCT116 cells. Nascent DNA was prepared from asynchronous cultures of HCT116 and Orc2$^{\Delta/-}$ cells, as described in Materials and Methods. Its abundance at the lamin B2, β-globin, and c-*myc* origins was quantified using real-time PCR for the peak (LB2, BG40.9, and *Myc*11) and negative (LB2C1, BG72, and *Myc*1) regions. Each bar represents three experiments, each done in duplicate, and one standard deviation. Statistically significant differences ($p < 0.05$) between the wild-type HCT116 and Orc2$^{\Delta/-}$ cells for the origin-containing regions are indicated with an asterisk.

-6 with replication origins (Figure 5) and resulted in a 3.4−4.5-fold decrease in origin activity (*31*), the effect of Orc2 deficiency on the activity of the LB2, BG40.9, and *Myc*11 origins was analyzed using Orc2$^{\Delta/-}$ hypomorphic cells. HsOrc2 associates with origins of replication throughout the cell cycle (our unpublished data) and is required for the stability of HsOrc3 (*18*). Thus, if the effect of Ku80 deficiency on DNA replication was mediated through the assembly of the ORC complex at origins, then a similar result would be expected in a cell line deficient for Orc2.

To assess origin activity in Orc2$^{\Delta/-}$ cells, nascent strand abundance at the lamin B2, β-globin, and c-*myc* origins was measured, using λ-exonuclease digested DNA, as described in Materials and Methods (*38*) (Figure 7). At the lamin B2 origin, LB2, nascent DNA was 4.5-fold more abundant in the wild-type HCT116 than Orc2$^{\Delta/-}$ cells (1.9×10^6 vs 4.2×10^5 molecules/20 μg of DNA, respectively, $p = 0.002$). In contrast, the abundance of nascent DNA at the control region, LB2C1, was similar in both cell lines (2.4×10^5 vs 1.9×10^5 molecules/20 μg of DNA for HCT116 and Orc2$^{\Delta/-}$ cells, respectively, $p = 0.717$). Similar results were observed for the other two origins examined. At the β-globin origin, nascent DNA abundance was 2.2-fold greater in the wild-type versus hypomorphic cells (1.75×10^6 vs 7.8×10^5 molecules/20 μg of DNA, respectively, $p = 0.028$), while its control region, BG72, displayed similar abundance in both cell lines (4×10^4 vs 5×10^4 molecules/20 μg of DNA in HCT116 and Orc2$^{\Delta/-}$ cells, respectively, $p = 0.938$). At the c-*myc* origin, *Myc*11, wild-type cells had 2.7-fold greater activity than hypomorphic cells (1.15×10^6 vs 4.2×10^5 molecules/20 μg of DNA, respectively, $p = 0.025$), while nascent DNA abundance at *Myc*1 was similar in both cell lines (2.8×10^5 vs 3.1×10^5 molecules/20 μg of DNA for HCT116 and Orc2$^{\Delta/-}$ cells, respectively, $p = 0.101$).

Comparison of nascent DNA abundance at the peak and negative control regions of each origin in wild-type HCT116 cells gives a measure of the quality of nascent DNA preparation (*46*). A ratio of 8−10-fold greater nascent DNA at the peak region relative to the negative control has been proposed to represent good nascent DNA preparations (*46*, *47*). Using λ-exonuclease-treated DNA, the peak region of the lamin B2 origin, LB2, was approximately 8-fold greater than its control region of LB2C1 (1.9×10^6 vs 2.4×10^5 molecules/20 μg of DNA, $p = 0.001$, respectively) (Figure 7); the β-globin origin, BG40.9, was approximately 44-fold greater than its control region, BG72 (1.75×10^6 vs 4×10^4 molecules/20 μg of DNA, $p = 0.001$, respectively), and the peak region of the c-*myc* origin, *Myc*11, was approximately 4-fold greater than the control, *Myc*1 (1.15×10^6 vs 2.8×10^5 molecules/20 μg of DNA, $p = 0.004$, respectively).

DISCUSSION

The human ORC complex is required for initiation of DNA replication and the loading of initiator proteins onto origins, including Cdc6, Cdt1, and the MCM hexameric complex (reviewed in ref *22*). Its DNA binding activity lacks sequence specificity in vitro, while in vivo, it specifically associates with DNA replication origins (*14*−*16*; Figures 5 and 6). Thus, it was proposed that another origin-binding protein may recruit HsORC to origins (*40*). In this study, the role of Ku in HsORC assembly at origins is examined, and the order of assembly of these two complexes is determined using Ku80- and Orc2-deficient cell lines.

Haplo-insufficient Ku80$^{+/-}$ cells were reported to have a prolonged doubling time and G_1 phase (*30*, *31*). Their decreased expression of Ku80 (Figure 1) resulted in a significant decrease of its association to chromatin (Figure 2), albeit to a lesser extent. This may reflect differences in the pools of DNA-bound and unbound Ku and suggests that Ku is more likely to be DNA bound than not. Indeed, measurements of nuclear GFP-tagged Ku mobility by

fluorescence photobleaching assay identified a 100-fold decrease in its diffusion relative to that predicted by its size (*48*). Analysis of the nuclear expression of HsOrc-2, -3, -4, and -6 did not reveal significant differences between the Ku80-deficient and wild-type cell lines (Figure 1), indicating that Ku does not regulate the expression or the stability of the HsOrc proteins. Furthermore, Ku80 deficiency did not have an effect on the association of the four HsOrc subunits with chromatin (Figure 2), most likely reflecting the emerging multiple functions of the HsOrc subunits, whereby they were found to interact with nonreplication proteins (*49*, *50*) and have been implicated in other functions than DNA replication, including transcriptional silencing (*50*−*53*). Alternatively, Ku80 deficiency may not have had an effect on the chromatin association of HsORC due to the latter's reported sequence-independent DNA binding activity (*14*, *15*).

Coimmunoprecipitation analyses indicated that the Ku heterodimer and the HsOrc-2, -3, -4, and -6 subunits are part of a complex, since they were brought down together (Figure 3). Ku and Orc2 were reported to coimmunoprecipitate in the presence of ethidium bromide (*24*), a DNA intercalating agent which disrupts DNA−protein interactions (*54*), indicating that their interaction is independent of DNA, but not necessarily a direct one.

Specific in vivo association of Ku and HsOrc proteins with the lamin B2, β-globin, and c-*myc* origins of DNA replication was demonstrated in cells synchronized to late G_1 (Figure 5), when assembly of the prereplication complex (pre-RC) takes place. As expected, the association of Ku80 with these origins was decreased in the $Ku80^{+/-}$ deficient cells (Figure 5; *31*). Interestingly, for all three origins examined, the association of HsOrc-3, -4, and -6 was also decreased, while that of HsOrc2 was not significantly affected. This indicated that loading of the HsOrc-3, -4, and -6 subunits preceded that of Ku. Alternatively, Ku may be involved in the stabilization of the interaction between the HsOrc-3, -4, and -6 subunits either with HsOrc-2 or with origin DNA. In fact, a previous study found that the yeast Ku homologue, HDF2, helped to stabilize the association of an ORC-like protein complex with *ARS*121 (*55*). Furthermore, a recent study found that Ku was involved in the stabilization of the interaction of PCNA with chromatin after ionizing radiation-induced DNA damage (*56*). Cdc6 was also identified as a stabilizer of the HsORC complex to DNA (*57*).

Since the association of HsOrc2 with chromatin was not affected by the deficiency of Ku80, the association of Ku80 with origins in $Orc2^{\Delta/-}$ hypomorphic cells was examined to determine the order of association of these two proteins. If HsOrc2 were required for the association of Ku80 with the origins, a deficiency in the association of HsOrc2 with them would lead to a deficiency in that of Ku80. Alternatively, if the two proteins bound independently of each other, a deficiency of one protein would not influence the origin association of the other. ChIP analysis in $Orc2^{\Delta/-}$ cells revealed an expected decrease in the association of HsOrc2 with all three origins examined (Figure 6), but the association of Ku80 was neither significantly nor consistently affected, indicating that HsOrc2 deficiency had no effect on the binding of Ku80 to the origins. Thus, HsOrc2 and Ku appear to bind to replication origins independently of each other. This is consistent with published data whereby Ku binds specifically to regions with homology to the A3/4 sequence (*23*, *28*), a version of the mammalian origin consensus (*27*), while HsORC binding does not seem to be sequence-specific, but rather biased toward A/T-rich regions (*14*, *15*).

Decreased origin activity has been observed in $Ku80^{+/-}$ cells (*31*). To determine whether this was mediated by a deficiency in HsORC complex assembly at replication origins, we tested the origin activities in $Orc2^{\Delta/-}$ hypomorphic cells, which likely suffer a similar decrease in HsORC association to origins. Using λ-exonuclease-digested DNA, the activities of the lamin B2, β-globin, and c-*myc* origins were found to be decreased in $Orc2^{\Delta/-}$ hypomorphic cells compared to wild-type HCT116 (Figure 7). Dhar et al. (*14*) showed that the expression of HsOrc3 was decreased in the $Orc2^{\Delta/-}$ hypomorphic cell line. Thus, in addition to the decrease in the association of HsOrc2 with origins in $Orc2^{\Delta/-}$ cells (Figure 6), the association of the other ORC subunits with these origins is likely to be decreased, thus compromising origin firing. Hence, it is plausible that the decrease in origin activity seen in $Ku80^{+/-}$ cells be due to decreased association of Ku with the origins, leading to a decrease in the assembly of the entire ORC complex at these origins.

The initial study examining origin activity in $Orc2^{\Delta/-}$ cells did not detect any differences between the hypomorphic and wild-type cells (*14*). The observed decrease here might be due to the different assays used for preparation of nascent DNA. In this study, the λ-exonuclease enzyme, which degrades DNA lacking an RNA primer, was used, leading to a decrease in background signal that may be generated by broken DNA. This ensured the preparation of high-quality nascent DNA, whereby the ratio of abundance of the peak (origin-containing) to negative control (nonorigin) regions ranged up to 44-fold in wild-type cells (Figure 7).

Use of real-time PCR allowed the quantification of the amount of DNA that was immunoprecipitated by each antibody. As exemplified in Figure 5A, more DNA was immunoprecipitated with anti-HsOrc-3 and -6 than with anti-HsOrc-2 and -4 antibodies at the LB2 region. This pattern, also seen for the BG40.9 and *Myc*11 origin regions (Figure 5B,C), is a reflection of the immunoprecipitation efficiencies of anti-HsOrc antibodies (Figure 3B) which may be affected by epitope availability for each antibody. Interestingly, the amount of the non-origin-containing DNA sequences, LB2C1, and to a lesser extent of *Myc*1, brought down by the anti-HsOrc antibodies is greater than that of NGS, likely reflecting the sequence-independent binding activity of the HsOrc proteins (*14*, *15*).

Similarities in primer efficiencies allowed comparisons between the different amplified regions. For example, in the ChIP analyses, the signals obtained for the LB2 and BG40.9 origin-containing regions were generally greater than those of *Myc*11 (Figure 6). This indicated that the LB2 and BG40.9 origins were active in a greater fraction of cells than the c-*myc* origin (Figure 7). Another consistent observation among all immunoprecipitates was that the amount of DNA for the nonorigin LB2C1 and *Myc*1 regions was greater than the BG72 region, likely a result of the greater distance between BG72 and BG40.9 (∼31 kb) than LB2C1 and LB2 (∼4 kb) or *Myc*1 and *Myc*11 (∼5.9 kb). This distance ensures that, after sonication, there are less immunoprecipitated DNA molecules carrying these negative regions.

Table 2: DNA Binding Sites for the Ku Heterodimer and Its Individual Subunits[a]

DNA binding protein	recognition element[b]	recognition sequence (5′ → 3′)	function	ref
Ku80	A3/4	CCTCAAATGGTCTCCAATTTTCCTTTGGCAAATTCC	DNA replication	*28*
Ku70	NRE1	ACCGGACTGAGAAAGAGAAAGACGAC	transcription repression	*28*
Ku80	Ku80 binding site	GAGAAA	transcription repression	*59*
Ku70/80	SRE	ATTT	transciption repression/Ig class switch recombination	*60*
Ku70/80	HIV-1 LTR	CTGAGAGAGAAGTGTTAGAGT	transcription repression	*61*
Ku70		WGATAR	transcription repression	*62*
Ku70/80	human UCE	CAGGTGTCCGTGTCGCGCGTCGCCTGGGCCGGCGGCG	transcription repression	*63*
Ku70	IAP	CTGCGCATGTGCCAAGGGTATCTTATGACT	transcription activator	*64*
Ku70/80	URE5	AAGTTCCACCCCTTTCCCTTTCATTCA	transcription repression	*65*
Ku70	HSE	CCCGAAACTGGAAGATTCTTGGCCC	transcription repression	*66*, *67*

[a] Summary of DNA binding sites for Ku, including the binding subunit(s), the name and sequence of the recognition elements, the function of the element, and the reference(s) from which the above information was derived. [b] Abbreviations of names of recognition elements: NRE-1 = negative regulatory element 1 of the murine mammary tumor virus long-terminal repeat (LTR); SRE = switch regulatory element; HIV-1 LTR = human Immunodeficiency virus 1 long-terminal repeat; UCE = upstream control element; IAP = LTRs of mouse intracisternal A-particle (IAP) proviral elements; URE5 = U5 repressive element; HSE = heat shock element.

Crystallization of the Ku heterodimer revealed the presence of a preformed ring through which double-stranded DNA ends could enter, thus providing the mechanism of the DNA end-binding activity of Ku (*58*). Although not evident in the crystal structure, several studies identified a sequence-specific DNA binding activity in Ku (*28*, *59*−*67*) and identified DNA sequences to which Ku binds (summarized in Table 2). Two possible explanations may be proposed for Ku's ability to bind these seemingly different sequences: first, Ku-interacting proteins may modulate its binding affinity to different sequences that contain a Ku-binding recognition motif, possibly by changing the conformation of Ku, and/or second, each of these sequences may be bound by both Ku and other protein(s), either individually or as part of a protein complex, each conferring upon Ku the ability to perform a distinct function. For example, although both A3/4 and NRE1 can be bound by Ku, only A3/4 can support DNA replication (*28*), while NRE1 represses transcription, suggesting the existence of distinct Ku-containing transcription and replication complexes. Alternatively, the observed specific binding of Ku to seemingly unrelated sequences might be achieved through its proposed binding of polypurine/polypyrimidine stretches (*61*).

The multifunctionality of Ku in DNA-related cellular activities as well as its display of both nonspecific and sequence-specific DNA binding, led to the speculation that Ku may be poised to display different activities, depending on the prevailing cellular conditions and/or requirements. Thus, its function might be a combination of all the individually ascribed roles, elicited by its physical presence on the DNA and the prevailing cellular requirements for either DNA repair, replication, telomere maintenance, transcriptional silencing, or recombination. Despite the fact that these activities generally take place in complexes that assemble on the nuclear matrix, no differences were observed in origin abundance in the nuclear matrix fractions of wild-type and Ku80$^{+/-}$ cells (unpublished data), indicating that Ku does not recruit origins to the nuclear matrix.

Overall, on the basis of the data in the present and previous studies, the following model is proposed (Figure 8): Ku and HsOrc2 bind to separate sequences at human DNA replication origins independently of each other. From the present data, it cannot be determined which of the two proteins binds first. However, upon binding, Ku facilitates the loading of

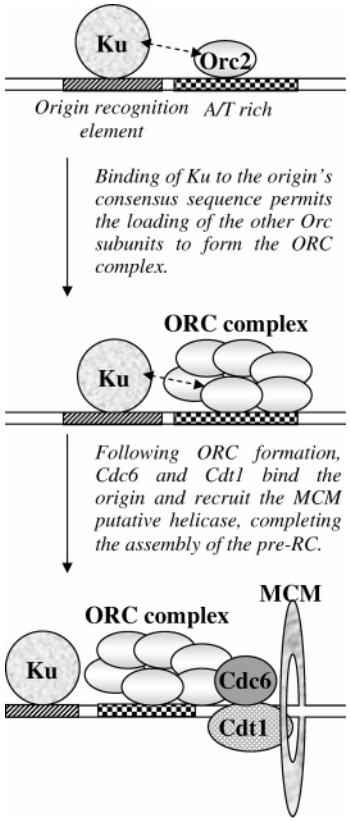

FIGURE 8: A model of the assembly of initiators of DNA replication at human replication origins. HsOrc2 and Ku bind to the A/T-rich region and an origin recognition element, respectively, independently of each other. Ku interacts with the HsOrc2 subunit (*24*; Figure 3) (indicated by the double-headed dashed arrow) and possibly modifies the DNA environment so as to allow binding of the other HsOrc subunits to HsOrc2 and assembly of the HsORC complex. This is followed by the binding of Cdc6, Cdt1, and the MCM2−7 complex, completing the assembly of the pre-RC and licensing the origin.

at least the HsOrc-3, -4, and -6 subunits. Although HsOrc-1 and -5 were not tested here, it had been previously shown that both subunits bind to form the HsORC complex after HsOrc-3 interacts with HsOrc-2 (*14*), thus inferring that the entire HsORC complex assembles after the binding of Ku to replication origins. Subsequently, Cdc6, Cdt1, and the MCM2−7 complex bind to the origin and license it to initiate DNA replication (reviewed in ref *22*). The observation that

Ku coimmunoprecipitates with the Orc subunits indicates that, at some point in time, they form a DNA replication complex, possibly following origin binding.

Several possible roles for Ku in DNA replication can be postulated, including a prerequisite requirement to be present at origins in case of DNA damage. Alternatively, it may be required to repress DNA transcription, thus allowing DNA replication to initiate (*59*−*67*) and preventing head-on collision of the transcription and replication machineries. In support of this notion, Ku was found to associate with TTF1 (*t*ranscription *t*ermination *f*actor 1) at the mouse rDNA origin (*68*). Finally, Ku may be required to unwind DNA through its helicase activity (*69*), thus allowing other DNA replication proteins to bind.

In conclusion, this is the first study to analyze the order of Ku binding at replication origins in relation to the HsOrc proteins. Studies are in progress to determine whether the loading of the HsOrc-3, -4, and -6 subunits onto origins results from direct interactions with the Ku heterodimer or is due to indirect modification(s) of the chromatin structure by Ku.

ACKNOWLEDGMENT

We thank Dr. Anindya Dutta for critical reading of the manuscript.

REFERENCES

1. Gilbert, D. M. (1986) Temporal order of replication of *Xenopus laevis* 5S ribosomal RNA genes in somatic cells, *Proc. Natl. Acad. Sci. U.S.A. 83*, 2924−2928.
2. Goldman, M. A., Holmquist, G. P., Gray, M. C., Gaston, L. A., and Nag, A. (1984) Replication timing of genes and middle repetitive sequences, *Science 224*, 686−692.
3. Pierron, G., Durica, D. S., and Sauer, H. W. (1984) Invariant temporal order of replication of the four actin gene loci during the naturally synchronous mitotic cycles of *Physarum polycephalum*, *Proc. Natl. Acad. Sci. U.S.A. 81*, 6393−6397.
4. Jalouzot, R., Toublan, B., Wilhelm, M. L., and Wilhelm, F. X. (1985) Replication timing of the H4 histone genes in *Physarum polycephalum*, *Proc. Natl. Acad. Sci. U.S.A. 82*, 6475−6479.
5. Huberman, J. A., and Riggs, A. D. (1968) On the mechanism of DNA replication in mammalian chromosomes, *J. Mol. Biol. 32*, 327−341.
6. Hand, R. (1978) Eucaryotic DNA: organization of the genome for replication, *Cell 15*, 317−325.
7. Zannis-Hadjopoulos, M., and Price, G. (1998) Regulatory parameters of DNA replication, *Crit. Rev. Eukaryotic Gene Expression 8*, 81−106.
8. Zannis-Hadjopoulos, M., and Price, G. B. (1999) Eukaryotic DNA replication, *J. Cell. Biochem., Suppl. 32/33*, 1−14.
9. Vogelauer, M., Rubbi, L., Lucas, I., Brewer, B. J., and Grunstein, M. (2002) Histone acetylation regulates the time of replication origin firing, *Mol. Cell 10*, 1223−1233.
10. Bell, S. P., and Stillman, B. (1992) ATP-dependent recognition of eukaryotic recognition of origins of DNA replication by multiprotein complex, *Nature 357*, 128−134.
11. Ruiz, M. T., Pearson, C. E., Nielsen, T., Price, G. B., and Zannis-Hadjopoulos, M. (1995) Cofractionation of HeLa cell replication proteins with *ors*-binding activity, *J. Cell. Biochem. 58*, 221−236.
12. Ruiz, M. T., Matheos, D., Price, G. B., and Zannis-Hadjopoulos, M. (1999) OBA/Ku86: DNA binding specificity and involvement in mammalian DNA replication, *Mol. Biol. Cell 10*, 567−580.
13. Klemm, R. D., Austin, R. J., and Bell, S. P. (1997) Coordinate binding of ATP and origin DNA regulates the ATPase activity of the origin recognition complex, *Cell 88*, 493−502.
14. Dhar, S. K., Delmolino, L., and Dutta, A. (2001) Architecture of the human origin recognition complex, *J. Biol. Chem. 276*, 29067−29071.
15. Vashee, S., Cvetic, C., Lu, W., Simancek, P., Kelly, T. J., and Walter, J. C. (2003) Sequence-independent DNA binding and replication initiation by the human origin recognition complex, *Genes Dev. 17*, 1894−1908.
16. Ladenburger, E. M., Keller, C., and Knippers, R. (2002) Identification of a binding region for human origin recognition complex proteins 1 and 2 that coincides with an origin of DNA replication, *Mol. Cell. Biol. 22*, 1036−1048.
17. Keller, C., Ladenburger, E. M., Kremer, M., and Knippers, R. (2002) The origin recognition complex marks a replication origin in the human TOP1 gene promoter, *J. Biol. Chem. 277*, 31430−31440.
18. Dhar, S. K., Yoshida, K., Machida, Y., Khaira, P., Chaudhuri, B., Wohlschlegel, J. A., Leffak, M., Yates, J., and Dutta, A. (2001) Replication from oriP of Epstein−Barr virus requires human ORC and is inhibited by geminin, *Cell 106*, 287−296.
19. Chaudhuri, B., Xu, H., Todorov, I., Dutta, A., and Yates, J. L. (2001) Human DNA replication initiation factors, ORC and MCM, associate with oriP of Epstein−Barr virus, *Proc. Natl. Acad. Sci. U.S.A. 98*, 10085−10089.
20. Schepers, A., Ritzi, M., Bousset, K., Kremmer, E., Yates, J. L., Harwood, J., Diffley, J. F., and Hammerschmidt, W. (2001) Human origin recognition complex binds to the region of the latent origin of DNA replication of Epstein−Barr virus, *Embo J. 20*, 4588−4602.
21. Ritzi, M., Tillack, K., Gerhardt, J., Ott, E., Humme, S., Kremmer, E., Hammerschmidt, W., and Schepers, A. (2003) Complex protein-DNA dynamics at the latent origin of DNA replication of Epstein−Barr virus, *J. Cell Sci. 116*, 3971−3984.
22. Zannis-Hadjopoulos, M., Sibani, S., and Price, G. B. (2004) Eukaryotic replication origin binding proteins, *Front. Biosci. 9*, 2133−2143.
23. Novac, O., Matheos, D., Araujo, F. D., Price, G. B., and Zannis-Hadjopoulos, M. (2001) In vivo association of Ku with mammalian origins of DNA replication, *Mol. Biol. Cell 12*, 3386−3401.
24. Matheos, D., Ruiz, M. T., Price, G. B., and Zannis-Hadjopoulos, M. (2002) Ku antigen, an origin-specific binding protein that associates with replication proteins, is required for mammalian DNA replication, *Biochim. Biophys. Acta 1578*, 59.
25. Matheos, D., Novac, O., Price, G. B., and Zannis-Hadjopoulos, M. (2003) Analysis of the DNA replication competence of the xrs-5 mutant cells defective in Ku86, *J. Cell Sci. 116*, 111−124.
26. Tuteja, R., and Tuteja, N. (2000) Ku autoantigen: a multifunctional DNA binding protein, *Crit. Rev. Biochem. Mol. Biol. 35*, 1−33.
27. Price, G. B., Allarakhia, M., Cossons, N., Nielsen, T., Diaz-Perez, M., Friedlander, P., Tao, L., and Zannis-Hadjopoulos, M. (2003) Identification of a cis-element that determines autonomous DNA replication in eukaryotic cells, *J. Biol. Chem. 278*, 19649−19659.
28. Schild-Poulter, C., Matheos, D., Novac, O., Cui, B., Giffin, W., Ruiz, M. T., Price, G. B., Zannis-Hadjopoulos, M., and Hache, R. J. (2003) Differential DNA binding of ku antigen determines its involvement in DNA replication, *DNA Cell Biol. 22*, 65−78.
29. Nussenzweig, A., Chen, C. H., Soares, V. D., Sanchez, M., Sokol, K., Nussenzweig, M. C., and Li, G. C. (1996) Requirement for Ku80 in growth and immunoglobulin V(D)J recombination, *Nature 382*, 551−555.
30. Li, G., Nelsen, C., and Hendrickson, E. A. (2002) Ku86 is essential in human somatic cells, *Proc. Natl. Acad. Sci. U.S.A. 99*, 832−837.
31. Sibani, S., Price, G. B., and Zannis-Hadjopoulos, M. (2005) Decreased origin usage and initiation of DNA replication in haploinsufficient HCT116 Ku80$^{+/-}$ cells, *J. Cell Sci.* (in press).
32. Vindelov, L. L. (1977) Flow microfluorometric analysis of nuclear DNA in cells from solid tumors and cell suspensions. A new method for rapid isolation and straining of nuclei, *Virchows Arch. B: Cell Pathol. 24*, 227−242.
33. Dignam, J. D., Lebovitz, R. M., and Roeder, R. G. (1983) Accurate transcription initiation by RNA polymerase II in a soluble extract from isolated mammalian nuclei, *Nucleic Acids Res. 11*, 1475−1489.
34. Tatsumi, Y., Tsurimoto, T., Shirahige, K., Yoshikawa, H., and Obuse, C. (2000) Association of human origin recognition complex 1 with chromatin DNA and nuclease-resistant nuclear structures, *J. Biol. Chem. 275*, 5904−5910.
35. Sambrook, J., Fritsch, E. F., and Maniatis, T. (1989) *Molecular Cloning*, 2nd ed., Cold Spring Harbor Laboratory Press, Cold Spring Harbor, NY.

36. Quintana, D., Hou, Z., Thome, K., Hendricks, M., Saha, P., and Dutta, A. (1997) Identification of HsORC4, a member of the human origin of replication recognition complex, *J. Biol. Chem. 272*, 28247−28251.
37. Novac, O., Alvarez, D., Pearson, C. E., Price, G. B., and Zannis-Hadjopoulos, M. (2002) The human cruciform binding protein, CBP, is involved in DNA replication and associates in vivo with mammalian replication origins, *J. Biol. Chem. 277*, 22.
38. Tao, L., Dong, Z., Leffak, M., Zannis-Hadjopoulos, M., and Price, G. (2000) Major DNA replication initiation sites in the c-myc locus in human cells, *J. Cell. Biochem. 78*, 442−457.
39. Hirt, B. (1967) Selective extraction of polyoma DNA from infected mouse cell cultures, *J. Mol. Biol. 26*, 365−369.
40. Bell, S. P., and Dutta, A. (2002) DNA replication in eukaryotic cells, *Annu. Rev. Biochem. 71*, 333−374.
41. Abdurashidova, G., Deganuto, M., Klima, R., Riva, S., Biamonti, G., Giacca, M., and Falaschi, A. (2000) Start sites of bidirectional DNA synthesis at the human lamin B2 origin, *Science 287*, 2023−2026.
42. Giacca, M., Zentilin, L., Norio, P., Diviacco, S., Dimitrova, D., Contreas, G., Perini, G., Weighardt, F., Riva, S., and Falaschi, A. (1994) Fine mapping of a replication origin of human DNA, *Proc. Natl. Acad. Sci. U.S.A. 91*, 7119−7123.
43. Kamath, S., and Leffak, M. (2001) Multiple sites of replication initiation in the human ss-globin gene locus, *Nucleic Acids Res. 29*, 809−817.
44. Kreitz, S., Ritzi, M., Baack, M., and Knippers, R. (2001) The human origin recognition complex protein 1 dissociates from chromatin during S phase in HeLa cells, *J. Biol. Chem. 276*, 6337−6342.
45. Mendez, J., and Stillman, B. (2000) Chromatin association of human origin recognition complex, cdc6, and minichromosome maintenance proteins during the cell cycle: assembly of prereplication complexes in late mitosis, *Mol. Cell Biol. 20*, 8602−8612.
46. DePamphilis, M. L. (1997) The search for origins of DNA replication, *Methods 13*, 211−219.
47. DePamphilis, M. L. (1999) Replication origins in metazoan chromosomes: fact or fiction?, *BioEssays 21*, 5−16.
48. Rodgers, W., Jordan, S. J., and Capra, J. D. (2002) Transient association of Ku with nuclear substrates characterized using fluorescence photobleaching, *J. Immunol. 168*, 2348−2355.
49. Dhar, S. K., and Dutta, A. (2000) Identification and characterization of the human ORC6 homolog, *J. Biol. Chem. 275*, 34983−34988.
50. Thome, K. C., Dhar, S. K., Quintana, D. G., Delmolino, L., Shahsafaei, A., and Dutta, A. (2000) Subsets of human origin recognition complex (ORC) subunits are expressed in non-proliferating cells and associate with non-ORC proteins, *J. Biol. Chem. 275*, 35233−35241.
51. Sutton, A., Heller, R. C., Landry, J., Choy, J. S., Sirko, A., and Sternglanz, R. (2001) A novel form of transcriptional silencing by Sum1-1 requires Hst1 and the origin recognition complex, *Mol. Cell. Biol. 21*, 3514−3522.
52. Iizuka, M., and Stillman, B. (1999) Histone acetyltransferase HBO1 interacts with the ORC1 subunit of the human initiator protein, *J. Biol. Chem. 274*, 23027−23034.
53. Fox, C. A., Ehrenhofer-Murray, A. E., Loo, S., and Rine, J. (1997) The origin recognition complex, SIR1, and the S phase requirement for silencing, *Science 276*, 1547−1551.
54. Lai, J. S., and Herr, W. (1992) Ethidium bromide provides a simple tool for identifying genuine DNA-independent protein associations, *Proc. Natl. Acad. Sci. U.S.A. 89*, 6958−6962.
55. Shakibai, N., Kumar, V., and Eisenberg, S. (1996) The Ku-like protein from *Saccharomyces cerevisiae* is required *in vitro* for the assembly of a stable multiprotein complex at a eukaryotic origin of replication, *Proc. Natl. Acad. Sci. U.S.A. 93*, 11569−11574.
56. Park, S. J., Ciccone, S. L., Freie, B., Kurimasa, A., Chen, D. J., Li, G. C., Clapp, D. W., and Lee, S. H. (2004) A positive role for the Ku complex in DNA replication following strand break damage in mammals, *J. Biol. Chem. 279*, 6046−6055.
57. Harvey, K. J., and Newport, J. (2003) Metazoan origin selection: origin recognition complex chromatin binding is regulated by CDC6 recruitment and ATP hydrolysis, *J. Biol. Chem. 278*, 48524−48528.
58. Walker, J. R., Corpina, R. A., and Goldberg, J. (2001) Structure of the Ku heterodimer bound to DNA and its implications for double-strand break repair, *Nature 412*, 607−614.
59. Xu, P., LaVallee, P. A., Lin, J. J., and Hoidal, J. R. (2004) Characterization of proteins binding to E-box/Ku86 sites and function of Ku86 in transcriptional regulation of the human xanthine oxidoreductase gene, *J. Biol. Chem. 279*, 16057−16063.
60. Schaffer, A., Kim, E. C., Wu, X., Zan, H., Testoni, L., Salamon, S., Cerutti, A., and Casali, P. (2003) Selective inhibition of class switching to IgG and IgE by recruitment of the HoxC4 and Oct-1 homeodomain proteins and Ku70/Ku86 to newly identified ATTT cis-elements, *J. Biol. Chem. 278*, 23141−23150.
61. Jeanson, L., and Mouscadet, J. F. (2002) Ku represses the HIV-1 transcription: identification of a putative Ku binding site homologous to the mouse mammary tumor virus NRE1 sequence in the HIV-1 long terminal repeat, *J. Biol. Chem. 277*, 4918−4924.
62. Camara-Clayette, V., Thomas, D., Rahuel, C., Barbey, R., Cartron, J. P., and Bertrand, O. (1999) The repressor which binds the −75 GATA motif of the GPB promoter contains Ku70 as the DNA binding subunit, *Nucleic Acids Res. 27*, 1656−1663.
63. Kuhn, A., Stefanovsky, V., and Grummt, I. (1993) The nucleolar transcription activator UBF relieves Ku antigen-mediated repression of mouse ribosomal gene transcription, *Nucleic Acids Res. 21*, 2057−2063.
64. Kim, D., Ouyang, H., Yang, S. H., Nussenzweig, A., Burgman, P., and Li, G. C. (1995) A constitutive heat shock element-binding factor is immunologically identical to the Ku autoantigen, *J. Biol. Chem. 270*, 15277−15284.
65. Okumura, K., Takagi, S., Sakaguchi, G., Naito, K., Minoura-Tada, N., Kobayashi, H., Mimori, T., Hinuma, Y., and Igarashi, H. (1994) Autoantigen Ku protein is involved in DNA binding proteins which recognize the U5 repressive element of human T-cell leukemia virus type I long terminal repeat, *FEBS Lett. 356*, 94−100.
66. Falzon, M., and Kuff, E. L. (1990) A variant binding sequence for transcription factor EBP-80 confers increased promoter activity on a retroviral long terminal repeat, *J. Biol. Chem. 265*, 13084−13090.
67. Falzon, M., Fewell, J. W., and Kuff, E. L. (1993) EBP-80, a transcription factor closely resembling the human autoantigen Ku, recognizes single- to double-strand transitions in DNA, *J. Biol. Chem. 268*, 10546−10552.
68. Wallisch, M., Kunkel, E., Hoehn, K., and Grummt, F. (2002) Ku antigen supports termination of mammalian rDNA replication by transcription termination factor TTF-−I, *Biol. Chem. 383*, 765−771.
69. Tuteja, N., Rahman, R., Tuteja, R., Ochem, A., Skopac, D., and Falaschi, A. (1994) Human DNA helicase II: a novel DNA unwinding enzyme identified as the autoantigen, *EMBO J. 13*, 4991−5001.

BI047327N